Journal of Electrotechnology, Electrical Engineering and Management (2023)
Clausius Scientific Press, Canada
DOI: 10.23977/jeeem.2023.060514
ISSN 2560-6697 Vol. 6 Num. 5

Simulation of Iron Core Proton Discrimination Capability in the HADAR Experiment

Xiaoyao Ma[1,2,a,*], Haijin Li[1,2,b,*], Liwu Liu[1,2,c], Shaozhang Zhao[1,2,d], Shang Sun[1,2,e], Qi Gao[1,2,f,*]

[1]Department of Physics, Faculty of Science, Tibet University, Lhasa, Tibet, China
[2]Department of Computing, Tibet University, Lhasa, Tibet, China
[a]3066797421@qq.com, [b]haijin_li1976@163.com, [c]liulw@ihep.ac.cn, [d]zhaosz@ihep.ac.cn, [e]sunlaoke@qq.com, [f]fbc1980@163.com
[*]Corresponding author

Keywords: Cosmic ray, CORSIKA, Component discrimination, Q-factor

Abstract: The research detailed in this paper focuses on an extensive simulation of the HADAR experiment's detection capabilities concerning iron cores and protons. Leveraging a sophisticated software package built on the CORSIKA simulation program, the study meticulously examined the distribution characteristics of secondary particles emitted by iron cores and protons. Discrimination between these primary cosmic rays was accomplished through the utilization of Hillas parameters and MRSW (Modified Hillas parameters - Mean Reduced Scaled Width) parameters. Additionally, a quantitative assessment was introduced in the form of the Q-factor to gauge the effectiveness of both discrimination methods.The obtained results showcase the HADAR experiment's remarkable proficiency in not only detecting but also distinguishing between iron cores and protons. Notably, the MRSW method emerged as highly effective, demonstrating significantly superior discrimination capabilities compared to the Hillas parameters. This advancement is pivotal for the HADAR experiment, providing researchers with a more robust and accurate tool for characterizing cosmic ray events.The successful discrimination achieved in this study contributes valuable insights to the broader field of astroparticle physics. The refined capabilities of the HADAR experiment open new avenues for investigating the intricate properties of cosmic rays, thereby advancing our understanding of high-energy astrophysical phenomena. These findings, presented in this paper, lay the groundwork for future research endeavors and underscore the HADAR experiment's significance in unraveling the mysteries of the cosmos.

1. Introduction

The study of the cosmic ray energy spectrum, particularly the energy spectra of various components, can effectively address the issues of cosmic ray origins, acceleration, and propagation. This is especially true for the study of heavy particle energy spectra. By tracing the abundance of heavy nuclei elements throughout cosmic history, one can indirectly investigate the evolutionary history of stars, which are the sources of heavy nuclei, examine the cosmic evolutionary process, and test existing theoretical models. However, the method of indirectly measuring cosmic rays

through the measurement of cascade showers induced in the atmosphere faces significant uncertainties in energy scale and resolution. Additionally, a limited understanding of the strong interactions between high-energy particles leads to considerable discrepancies in the measurements of the single-component energy spectra of cosmic rays by different ground-based experiments.

The Hillas parameter method plays a significant role in gamma/proton (γ/p) discrimination using Imaging Cherenkov Telescopes and is one of the key methods for existing IACTs (Imaging Atmospheric Cherenkov Telescopes) in γ/p discrimination. Due to the different development processes of hadronic showers from various cosmic ray components, theoretically, IACTs can also achieve discrimination between different heavy particle components of cosmic rays under the observation of atmospheric Cherenkov telescopes with certain precision. Some experiments have begun attempts in this direction, such as the WFCTA array of LHAASO, which utilizes direct Cherenkov light for cosmic ray heavy particle discrimination. HADAR (The High Altitude Detection of Astronomical Radiation) is a next-generation telescope in planning, which uses transmission mirrors instead of the traditional reflective mirrors in IACTs. This design significantly enhances the field of view (approximately 60 degrees for HADAR) and lowers the detection threshold, offering unparalleled advantages in the observation of transient sources. To fully explore the potential of HADAR, this paper takes the discrimination of cosmic ray iron (Fe) and protons (P) as an example. It investigates HADAR's cosmic ray heavy nuclei detection capabilities by simulating the effective area, angular resolution, and energy resolution for Fe and proton detection in HADAR, and applies the Hillas parameter method and its improved versions for cosmic ray heavy particle discrimination.

2. Simulation Parameter Settings

The HADAR experiment is a composite array consisting of four large-aperture wide-angle water lenses and surrounding scintillator detectors, primarily designed for observing Cherenkov light produced in the atmosphere by cosmic rays and gamma rays. The array structure is shown in Figure 1(a). The water lenses and the surrounding plastic scintillator array (Yangbajing Composite Array) work in conjunction to conduct observations, with the four water lenses arranged in a square with a spacing of 100 meters. Figure 1(b) presents the detailed design of a single wide-angle water lens, which mainly consists of a 5m diameter hemispherical spherical tank lens, a cylindrical metal tank, and an imaging system at the bottom. The lens primarily serves as a Cherenkov light collector. The tank, with a radius of 4m and a height of 7m, is filled with high-purity water to enhance the transmission of ultraviolet photons. The inside of the tank is lined with absorbent material, and the outside with insulating material. The imaging system, composed of 18,961 2-inch photomultiplier tubes, is arranged on the focal plane of the lens to digitize the imaging. The system is designed with a curved surface to capture photons entering at large angles and is supported by a stainless steel frame. The focal length of the lens is 6.8m. This water lens structure is designed to achieve a large observational field of view, as shown in Figure 1(b), where parallel light entering at the edge is focused at the edge of the imaging system, enabling a total field of view angle of 60 °. Moreover, the water lens, as a novel lens technology, uses cost-effective acrylic materials and high-purity water as its basic materials, making it relatively low-cost and easy to maintain.

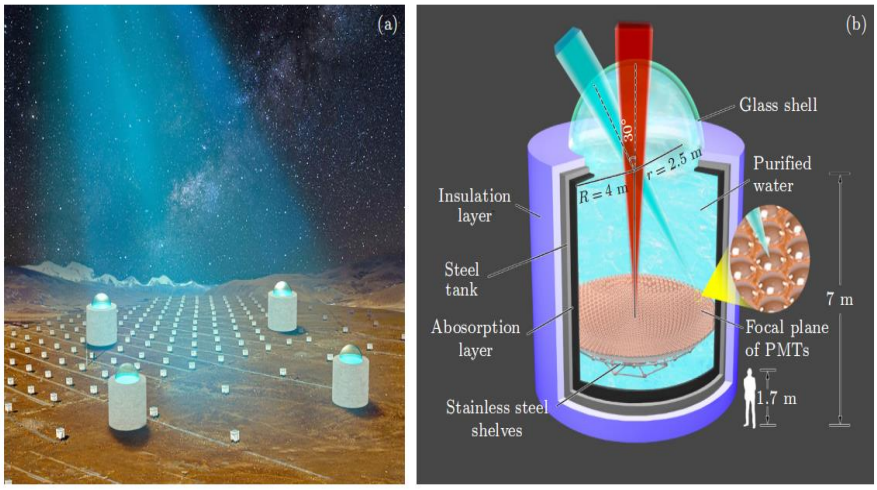

Figure 1: Schematic of the HADAR Array (a) Array layout; (b) Detailed structure of a single water lens.

During the simulation, the QGSJII-4 model was employed for the strong interactions of primary protons and iron cores in the CORSIKA simulation. The range of Cherenkov light radiation was set between 350 nm and 700 nm, consistent with the parameters in reference [1]. The energy range for primary particles was set at 30 GeV to 30 TeV for protons, and 500 GeV to 50 TeV for iron cores. The incident zenith angle was 10°, and the azimuthal angle ranged from 35° to 55°. In this simulation, the HADAR optical system consisted of four water lenses, each with a diameter of 5 meters, arranged in a square with a side length of 100 meters. The effective field of view was from -30° to 30°. The setup of the optical system, the imaging system, and the particle discrimination algorithm in the simulation program were consistent with those described in reference [2]. To ensure the reliability of the simulation results, the impact area for secondary particles was set to 800 × 800 m².

To ensure a similar number of Cherenkov photons produced by the two types of particles, the energy ratio of iron cores to protons can be calculated using the following equation:

$$\Delta = \frac{1.59^{\circ} Z}{E} \tag{1}$$

In the equation, Z represents the nuclear charge number of the incident particle, E is the energy of the incident particle, and Δ is the expected displacement of the particle. Based on this formula, the energy ratio of protons to iron cores is calculated to be 1:26.

3. Simulation of Basic Detection Properties of HADAR for Fe and P

To verify the reliability of the Fe/P energy range set in this simulation, the basic parameters such as effective area, angular resolution, and energy resolution for iron cores and protons in HADAR were simulated.

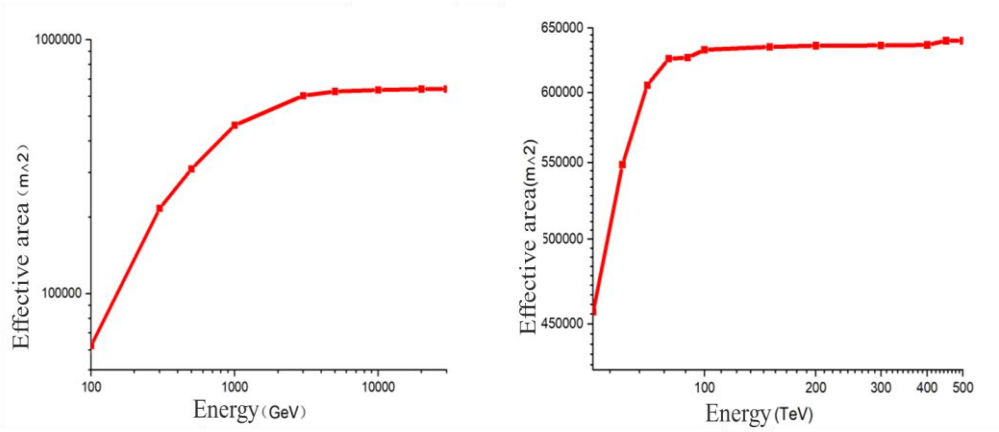

Figure 2: The change in effective area with energy for iron cores and protons at a 10 ° zenith angle incidence.

The effective area is defined as the product of the impact area of the air shower and the ratio of simulated events that trigger the detector and pass the selection criteria (consistent with the definitions in references [1] and [2]), and three parameters are introduced:

$$A_{eff} = S_{scatt} \times \frac{N_{cut}}{N_{total}} \tag{2}$$

Figure 2 presents the effective area at a 10 ° zenith angle incidence. The left graph shows the variation of the effective area for protons with energy, while the right graph shows the same for iron cores. As seen in Figure 2, the effective area increases with energy, with a rapid trend in the low-energy region and a more gradual trend in the high-energy region. Under the same conditions, the effective area for Fe is slightly smaller than that for P. Near the plateau region, the effective area for Fe is about 6.38×10^5 m^2, while for P, it is approximately 6.4×10^5 m^2.

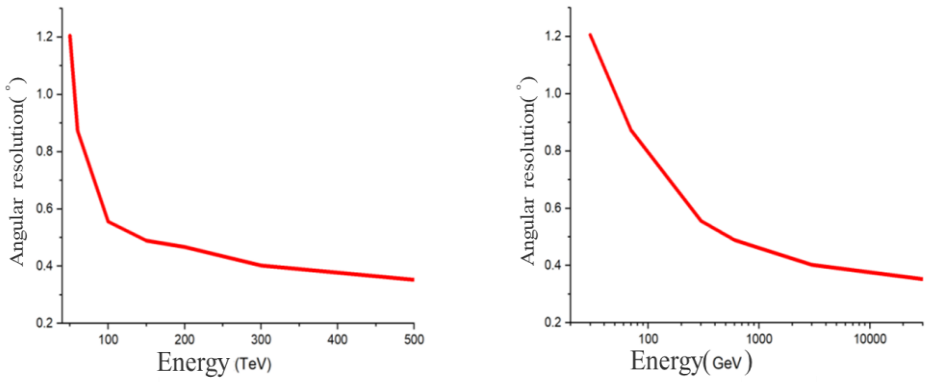

Figure 3: Variation in angular resolution with energy for iron cores and protons at a 10 ° zenith angle incidence.

The angular resolution simulation involved point sources, with particle types being Fe and P. The angular resolution was calculated by simulating the angular difference between the reconstructed direction and the true source direction (using a point spread function and taking the 68% containment radius). The incident angle in the simulation was 10 °. The angular resolution simulation results for iron cores and protons are shown in Figure 3, with the left graph depicting the

angular resolution variation with energy for iron cores, and the right for protons. As energy increases, the angular resolution capabilities for both iron cores and protons gradually improve, with a quick trend in the low-energy region and a more gradual trend in the high-energy region. The angular resolution capabilities of iron cores and protons are quite similar. HADAR's optimal angular resolution for Fe (500 TeV) is about 0.4 °, and for protons (30 TeV), it is also around 0.4 °, close to HADAR's angular resolution for gamma photons. This indicates that HADAR retains good angular resolution capabilities in Fe/P detection.

Energy reconstruction is achieved by detecting the number of secondary particles in the shower. The reconstructed energy, $E_{rec,}$ is related to the charge amount Q deposited in the detector, the incident angle θ, and the distance R from the telescope to the core position. Currently, there is no definitive formula to represent this relationship, and this paper adopts a look-up table method for energy reconstruction. The principle of the look-up table method can be found in reference [2]. Figure 4 presents the energy resolution graph after reconstruction, with the left graph for iron cores and the right graph for protons. As seen in Figure 4, the energy resolution improves with increasing energy, with a rapid trend in the low-energy region and a more gradual trend in the high-energy region. At 500 TeV, HADAR's energy resolution for Fe is approximately 22%, and the energy reconstruction for P is about 20%, indicating a good energy resolution."

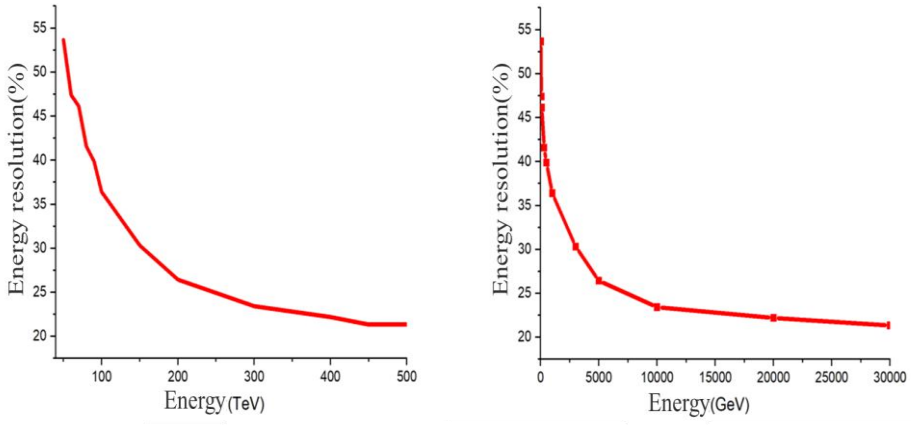

Figure 4: Variation in energy resolution for iron cores and protons with energy at a 10 °zenith angle incidence.

4. Fe/P Component Discrimination

4.1 Hillas Parameters and MRSW Method

The Hillas parameter method, proposed by A.M. Hillas in 1985, was originally developed for γ/P discrimination, aiming to filter out γ photons from a large background of protons. Due to the differences in the development processes of hadronic showers from various cosmic components, theoretically, HADAR can also achieve discrimination between different heavy particle components of cosmic rays under the observation of atmospheric Cherenkov telescopes with a certain precision.[3-7]

The Hillas parameters used in this paper are shown in Table 1. These include Dr: the distance between the event core and the array center, fLength: the major axis of the Hillas ellipse, fWidth: the minor axis of the Hillas ellipse, fSize the charge amount, fDistance: the distance between the image centroid and the telescope, fMiss: the perpendicular distance from the telescope array center to the image axis, and fAzwidth: the azimuthal width.

Table 1: Hillas parameters used in the study

Nev	tele	Dr	fLength	fWidth	fDelta	fSize
fMeanX	fMeanY	fDistance	fMiss	fAzwidth	fSinDelta	fCosDelta

According to the simulation results, the fWidth and fLength parameters can distinguish between Fe and P components to some extent. The fWidth parameter shows better discrimination performance compared to the fLength parameter, but it is still not ideal. Figure 5 shows the discrimination effects of fWidth and fLength parameters on iron cores and protons, respectively, on the left and right.

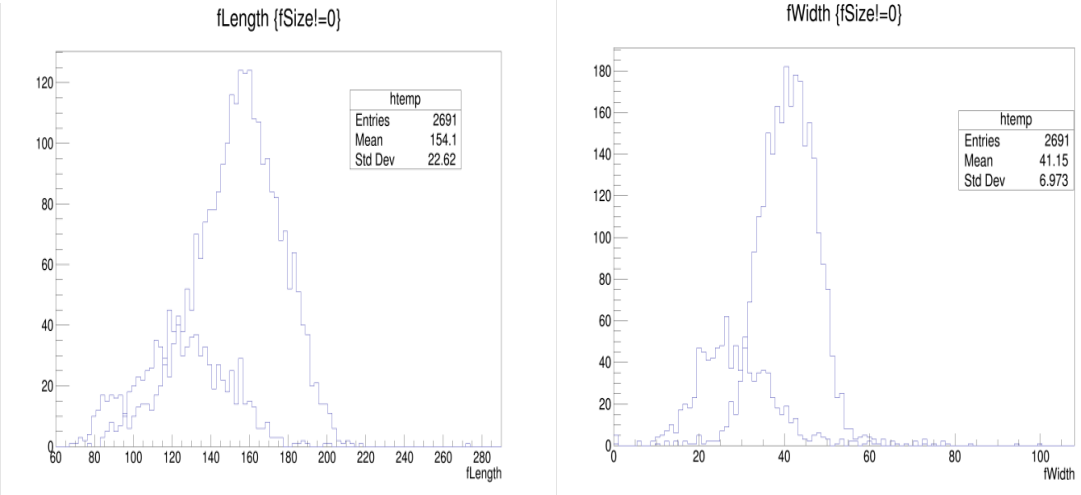

Figure 5: Discrimination of iron cores and protons using Hillas parameters.

The MRSW (Mean Reduced Scaled Width) parameter method is an improvement over the Hillas parameters. MRSW stands for Mean Reduced Scaled Width and can be calculated using the following formula:

$$\mathrm{MRSW} = \frac{1}{N_{tel}} \sum_{i \in N_{tel}} \frac{\mathrm{width}_i - <\mathrm{width}>_i}{\sigma_i} \tag{3}$$

In this method, width_i is the measured value, while $<\mathrm{width}>_i$ and σ_i are the expected value and the spread of the Hillas width (or length), respectively.[8-10]

The discrimination effectiveness of the MRSW parameter method is shown in Figure 6. The discrimination results of the MRSW method are superior to those of the Hillas parameter method. The effectiveness of different discrimination methods can be described using the Q-factor."

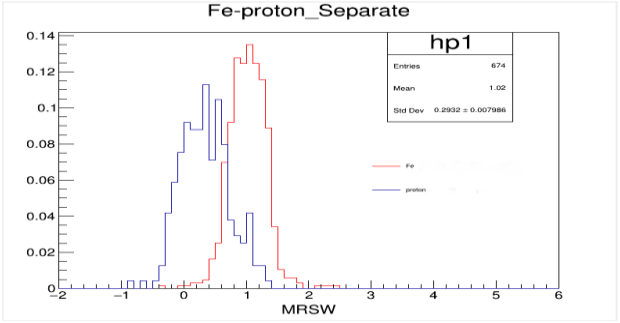

Figure 6: Discrimination of iron cores and protons using the MRSW method.

4.2 Q-factor

The Q-factor is defined as:

$$Q = \frac{\varepsilon_{survive}^{proton}}{\sqrt{\varepsilon_{survive}^{Fe}}} \tag{4}$$

$\varepsilon_{survive}^{proton}$ is the ratio of simulated protons after discrimination selection to the simulated protons before selection, also known as the survival rate of protons; $\varepsilon_{survive}^{Fe}$ is the ratio of simulated iron cores after discrimination selection to the simulated iron cores before selection, which is the survival rate of iron cores.[11-14]

The Q-factor is a function of energy, and a larger Q-factor indicates better discrimination effectiveness. When using a certain parameter for discrimination, if the Q-factor exceeds 2.0, it signifies that this parameter can effectively distinguish between components.

Figure 7 illustrates the variation of the Q-factor with different energies using three different selection parameters: (a) MRSW, (b) fWidth, and (c) fLength. As shown in Figure 7, the MRSW parameter demonstrates the best discrimination effectiveness. Regardless of the parameter, as energy increases, the Q-factor also increases, indicating improved discrimination effectiveness [15].

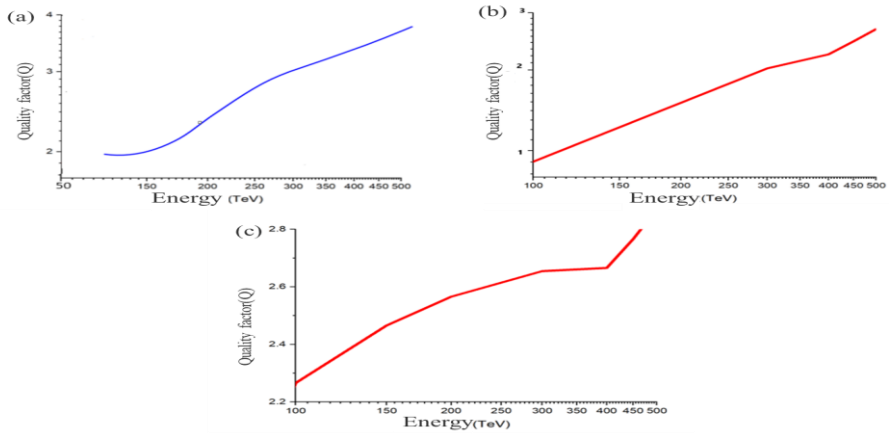

Figure 7: Relationship between the quality factor and energy in the HADAR experiment.

5. Conclusion

Using a software package based on the CORSIKA simulation program, the detection capabilities of the HADAR experiment for iron cores and protons were simulated. The distribution characteristics of secondary particles from iron cores and protons were utilized, employing Hillas parameters and MRSW (Modified Hillas parameters - Mean Reduced Scaled Width) for the discrimination of two types of primary cosmic rays. Additionally, the Q-factor was introduced to assess the discrimination effectiveness of these methods. The results show that HADAR has certain detection and discrimination capabilities for iron cores (50 TeV - 500 TeV) and protons (30 GeV - 30 TeV). As the energy increases, the effective area, angular resolution, and energy reconstruction resolution improve. The Hillas parameters and the improved MRSW parameters can be used to distinguish between Fe/P, with the discrimination effectiveness of the MRSW parameters

significantly superior to that of the Hillas parameters, and the discrimination capability noticeably increasing with higher energies. The introduction of neural networks and deep learning methods could further enhance HADAR's discrimination capabilities for cosmic ray heavy nuclei such as Fe/P.

References

[1] Zhao Litao. Research on improvement of heavy component identification of cosmic rays based on direct Cherenkov light . Liaoning University, 2019.

[2] Xin Guangguang. Experimental Performance of Radiation Detection of High altitude celestial bodies and Simulation of Very High Energy gamma Ray detection . Wuhan University, 2022.

[3] Zhao Litao, Ma Lingling, Zhang Shoushan, et al. Simulation of heavy component identification of cosmic rays by direct Cherenkov light . Nuclear Electronics and Detection Technology, 2017, 37(12): 1168-1173.

[4] Qu Xiaobo, Feng Cunfeng, Zhang Xueyao, et al. Determination of iron nuclei in the primary cosmic rays in the knee region by multi-scale analysis . Journal of Shandong University (Science Edition), 2008(05): 19-23.

[5] Wang Yudong, Wang Zhonghai, Zhou Rong, et al. Identification of cosmic ray components in "knee region" by CORSIKA simulation . Nuclear Electronics and Detection Technology, 2019, 39(05): 567-572.

[6] Aharonian F, An Q, Axikegu, et al. Calibration of the Air Shower Energy Scale of the Water and Air Cherenkov Techniques in the LHAASO experiment, Phys. Rev. D, 2021, 104(6): 062007.

[7] Bartoli B, Bernardini P, Bi X J, et al. Observation of the cosmic ray moon shadowing effect with the ARGO-YBJ experiment, Phys. Rev. D, 2011, 84(2): 022003.

[8] Bi B Y, Zhang S S, Cao Z, et al. Performance of SiPMs and pre-amplifier for the wide field of view Cherenkov telescope array of LHAASO, Nucl. Instrum. Meth. A, 2018, 899, 94-100.

[9] Zhang S S, Bai Y X, Cao Z et al. Properties and performance of two wide field of view Cherenkov/fluorescence telescope array prototypes, Nucl. Instrum. Meth. A, 2011, 629 (11): 57- 65.

[10] Yoon Y S, Anderson T, Barrau A, et al. Proton and Helium Spectra from the CREAM-III Flight, Astrophys. J., 2017, 839:5.

[11] Yin L Q, Zhang S S, Bi B Y, et al. Accurate Measurement of the Cosmic Ray Proton Spectrum from 100TeV to 10PeV with LHAASO. 35th International Cosmic Ray Conference, 2017.

[12] Gough M P. A proposed direct measurement of 1014eV iron primaries. J. Phys. G: Nucl. Phys., 1976, 2: 965-969.

[13] Kieda D B, Swordy S P, and Wakely S P. A high-resolution method for measuring cosmic ray composition beyond 10 TeV. Astropart. Phys., 2001, 15(3): 287-303.

[14] Corbato S C. The cosmic-ray energy spectrum observed by the Fly's Eye. Astrophys. J., 1994, 424:491-502.

[15] Qian Xiangli, Sun Huiying, Chen Tianlu, Feng Youliang, Gao Qi, Gou Quanbu, Guo Yiqing, Hu Hongbo, Kang Mingming, Li Haijin, Liu Cheng, Liu Maoyuan, Liu Wei, Qiao Bingqiang, Wang Xu, Wang Zhen, Xin Guangguang, Yao Yuhua, Yuan Qiang, Zhang Yi. Prospective study on observations of gamma-ray emission from active galactic nuclei using the HADAR experiment. Acta Phys. Sin. Vol. 72, No. 4 (2023) 049501